Low Reynolds Number Developing Flows

BERNARD ATKINSON, M. P. BROCKLEBANK, C. C. H. CARD, and J. M. SMITH

University College of Swansea, Swansea, Wales

Equations are given that relate the entrance length to Reynolds number for pipe and channel geometries with a flat velocity profile as the initial condition. These equations are linear combinations of the creeping flow and boundary layer solutions. The former is obtained by minimization of the viscous dissipation using the finite element method. The equation for the pipe entrance is shown to be in good agreement with experimental data.

The entrance region for laminar flow has received considerable attention in recent years. Not only is such study of importance for industrial and viscometric applications, but also as a simple developing flow it provides a useful vehicle for the evolution and evaluation of numerical solution procedures for nonlinear partial differential equations, for example, the Navier-Stokes equations. In consequence, the restrictions imposed on the solution by use of the Prandtl boundary-layer hypothesis have been overcome and, in principle, it is now possible to achieve a solution for all Reynolds numbers and boundary conditions.

The early numerical solutions were obtained by Bodoia and Osterle (*1*) for parallel plates, and Hornbeck (*2*) for pipes, both using a flat velocity profile as an initial condition and applying the boundary-layer hypothesis to yield initial value problems. The velocity and pressure fields were then obtained by finite difference procedures (*3*). These studies have been extended to the lower Reynolds number region where the problem is of the boundary value type, by Wang and Longwell (*4*) in the case of parallel plates and for pipes by Vrentas, Duda, and Bargeron (*5*). In the former, solutions are presented at a Reynolds number of 300 using both the flat velocity profile (Figure 1) and the stream-tube (Figure 2) as the initial condition, whereas in the latter, the stream-tube condition was used exclusively at Reynolds numbers of 0, 1, 50, 150, and 250.

The significant features of these solutions lie in the transport of vorticity upstream of the tube entrance when using the stream-tube condition (*4, 5*), the way the entrance length varies with Reynolds number (*5*), the finite entrance length at zero Reynolds number (*5*), and the fact that the maxima are predicted in the velocity profiles at locations other than the center line (*4*).

The associated experimental investigations, all in pipes, due to Nikuradse (*6*), Reshotko (*7*), and Pfenninger (*8*) are discussed by Atkinson, Kemblowski, and Smith (*9*), who have confirmed beyond reasonable doubt the high Reynolds number asymptote of the Navier-Stokes equations applied to entrance region problems.

Experimentally, one of two methods is used in an attempt to produce an acceptable approximation to a flat velocity profile for use as an initial condition. These are the type of device developed by Atkinson, et al. (*9*) and the conical entrance section (*7, 8*).

In view of the computations of Vrentas, et al. (*5*) application of the latter method is questionable at low Reynolds numbers because of the upstream axial diffusion of vorticity. A further alternative would be to locate the pipe entrance in a large volume of liquid in an approximation to the stream-tube situation. The limitation in this case would be the upstream vorticity transport from the external surfaces of the pipe.

A convenient integral measurement of a developing flow field is the entrance length, that is the downstream position at which the center line velocity attains an arbitrarily selected fraction of its final value.

The velocity field obtained from the Navier-Stokes equations applied to the pipe entry problem may be expressed as:

$$U = f(R, Z, N_{Re}) \tag{1}$$

or for the center line velocity:

$$U_{C/L} = f(Z, N_{Re}) \tag{2}$$

Since the final dimensionless center line velocity is 2, the entrance length may be defined as any specified

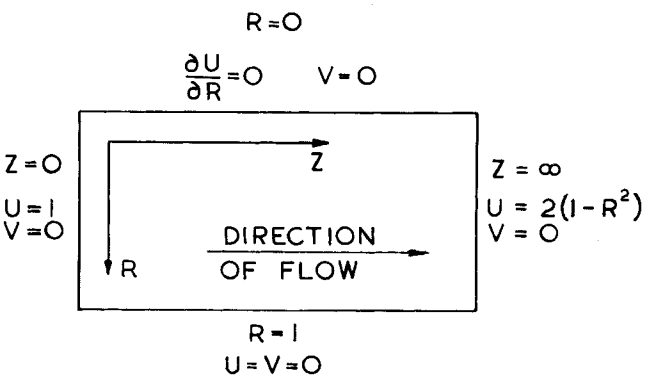

Fig. 1. The flat velocity profile initial condition.

fraction of this asymptote. At this position Equation (2) becomes:

$$Z_e = f(N_{Re}) \tag{3}$$

The boundary-layer approximation to the problem indicates that Equation (3) is linear. The results of Vrentas, et al. (5) for the stream tube initial condition confirm that the boundary-layer solution is the high Reynolds number asymptote. At low values the relationship is more complex (Figure 9) and at zero Reynolds number a finite entrance length might be anticipated.

CREEPING FLOW (Re → 0)

It has been suggested previously that the only realistic experimental initial condition at low Reynolds numbers is the generation of a flat velocity profile at a known position within the conduit. Any other condition would lead to indeterminate axial diffusion of vorticity. Thus the low Reynolds number asymptote of Equation (3) is required for the boundary conditions given on Figure 1. This asymptote may be obtained by using the fact that the extent of viscous dissipation for a flow whose inertia terms may be neglected, that is creeping flow, is finite, unique and a minimum for a given set of boundary conditions (*10* to *12*).

The local viscous dissipation for axisymmetric, incompressible flow when expressed dimensionlessly in cylindrical coordinates is given by (*13*):

$$\left(\frac{\mu\bar{u}^2}{a^2}\right)\left[2\left\{\left(\frac{\partial V}{\partial R}\right)^2+\left(\frac{V}{R}\right)^2+\left(\frac{\partial U}{\partial Z}\right)^2\right\}+\left\{\frac{\partial V}{\partial Z}+\frac{\partial U}{\partial R}\right\}^2\right] \tag{4}$$

A dimensionless stream function may be defined:

$$\psi = -\frac{1}{\bar{u}a^2}\int_o^a ur\,dr \tag{5}$$

$$U = -\frac{1}{R}\frac{\partial\psi}{\partial R};\quad V = \frac{1}{R}\frac{\partial\psi}{\partial Z} \tag{6}$$

Substituting Equation (6) into Equation (4) a function F is obtained such that

$$F = \frac{1}{R^4}\left(\frac{\partial\psi}{\partial R}\right)^2+\frac{4}{R^4}\left(\frac{\partial\psi}{\partial Z}\right)^2+\frac{1}{R^2}\left[\left(\frac{\partial^2\psi}{\partial R^2}\right)^2+\left(\frac{\partial^2\psi}{\partial Z^2}\right)^2\right]+\frac{4}{R^2}\left(\frac{\partial^2\psi}{\partial R\partial Z}\right)^2-\frac{2}{R^3}\frac{\partial^2\psi}{\partial R^2}\frac{\partial\psi}{\partial R}+\frac{2}{R^3}\frac{\partial^2\psi}{\partial Z^2}\frac{\partial\psi}{\partial R}$$

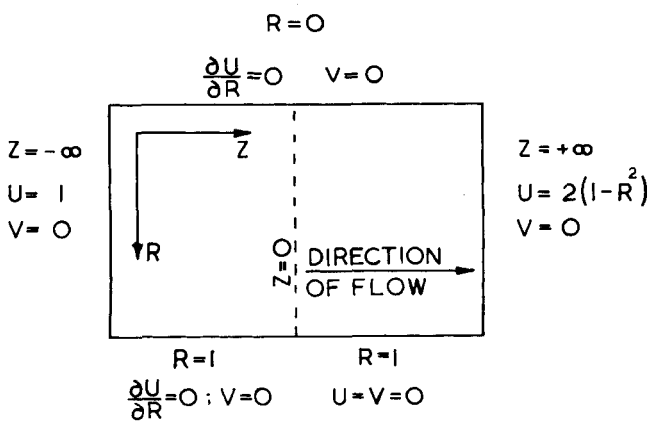

Fig. 2. The stream-tube initial condition.

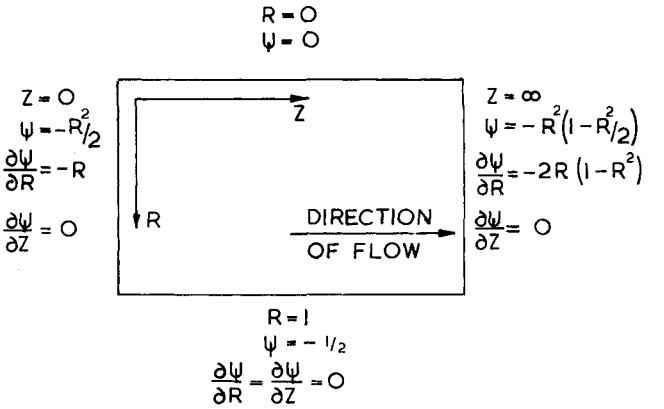

Fig. 3. The boundary value problem.

$$-\frac{4}{R^3}\frac{\partial^2\psi}{\partial Z\partial R}\frac{\partial\psi}{\partial Z}-\frac{2}{R^2}\frac{\partial^2\psi}{\partial Z^2}\frac{\partial^2\psi}{\partial R^2} \tag{7}$$

The problem reduces to the variational one of minimizing the integral of F over the flow field with

$$\frac{\partial}{\partial\psi}\iiint F(\psi)d(volume) = 0 \tag{8}$$

the boundary conditions given on Figure 3.

A numerical procedure that may be applied to such a mathematical problem has been devised for use in structural mechanics (*14*) and in that context has been developed by Zienkiewicz (*15*). This technique has been applied to the entrance region problem. The particular power of this method lies in the ease with which boundary conditions, and especially different boundary locations, may be treated as input data rather than requiring program modification.

PRINCIPLES OF THE FINITE ELEMENT METHOD

The solution domain is divided into a mesh, using finer spacing where the gradients are known to be large or additional detail is required. The vertexes of the mesh are referred to as *nodes* and the enclosed areas *elements*. These elements may have any arbitrary shape, though only the triangle and quadrilateral have been investigated to any extent.

The dependent variable in the problem (P) at any position X, Y is then related to nodal variables at each of the three nodes that form the element in which the position X, Y is located. For example, P and its derivatives with respect to the coordinates that is $\partial P/\partial X$ and $\partial P/\partial Y$, may be used as the nodal variables.

$$P = f_1\left[P_i, \frac{\partial P}{\partial X_i}, \frac{\partial P}{\partial Y_i}\right] \tag{9}$$

where $i = 1, 2, 3$ for a triangular element. Equation (9) is called the *shape function* and generally takes the form of a linear combination of the nodal variables.

The coefficients in Equation (9) depend on the position within the element at which it is desired to evaluate P together with the nodal coordinates. In practice, the most satisfactory way of locating such a position for a triangular element is an internal coordinate system called *area coordinates* (Figure 4). Any point within the triangle may be specified by:

$$E_1 = A_1/A;\quad E_2 = A_2/A;\quad E_3 = A_3/A$$
$$A = A_1 + A_2 + A_3 \tag{10}$$

Equation (9) and its derivatives are then substituted into the function $F(P)$ whose integral it is desired to minimize:

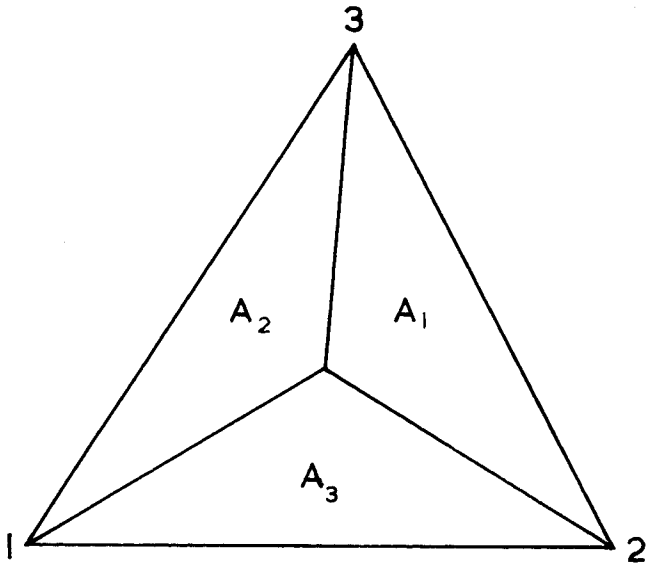

Fig. 4. Area Coordinates.

$$F(P) = f_2\left[P_i, \frac{\partial P}{\partial X_i}, \frac{\partial P}{\partial Y_i}\right] \tag{11}$$

$i = 1, 2, 3$ for a triangular element.

Integration of Equation (11) over the area of an element provides the contribution of that element to the total integral

$$\sum_{n=1}^{K} \iint_{A_n} F(P)\,d(area) \tag{12}$$

where n is the element number and K the total number of elements.

Differentiation of the contribution of each element in turn with respect to each of the nine nodal variables associated with an element results in nine independent relationships per element.

$$\frac{\partial}{\partial\ (nodal\ variable)} \iint_{A_n} F(P)\,d(area) \tag{13}$$

The sum of the relationships described by Equation (13) for a particular nodal variable over the whole field provides the total variation of the integral of $F(P)$ with respect to a given nodal variable. This variation must be zero for the integral of $F(P)$ to be a minimum.

$$\sum_{n=1}^{K} \frac{\partial}{\partial\ (nodal\ variable)} \iint_{A_n} F(P)\,d(area) = 0 \tag{14}$$

If Equation (14) is applied to all interior nodal variables, substitution of the boundary conditions and rearrangement results in a nonsingular system of linear equations in which the unknowns are the nodal variables and the coefficients are related to the nodal coordinates. This system of equations is then solved to obtain the complete set of nodal variables.

APPLICATION TO THE ENTRANCE REGION PROBLEM

A comprehensive discussion of the application of the finite element method to creeping flow problems is given by Card (*16*). The shape function [Equation (9)] will represent quadratic functions exactly, cubic functions fairly accurately and quartic functions inexactly. For the flow field associated with Figure 3 it can be seen that there is a region with quartic dependence. This may be reduced by defining a new variable:

$$B = \frac{\psi}{R^2} \tag{15}$$

In terms of this new variable the nodal variables are:

$$B;\quad \partial B/\partial R;\quad \partial B/\partial Z \tag{16}$$

and are related to ψ by

$$\frac{\partial B}{\partial R} = \frac{1}{R^2}\frac{\partial \psi}{\partial R} - 2\frac{\psi}{R^3}$$
$$\frac{\partial B}{\partial Z} = \frac{1}{R^2}\frac{\partial \psi}{\partial Z} \tag{17}$$

The Functional

Equation (7) may be transformed in terms of the new variable using the relationships:

$$\frac{\partial \psi}{\partial R} = 2RB + R^2\frac{\partial B}{\partial R}$$
$$\frac{\partial \psi}{\partial Z} = R^2\frac{\partial B}{\partial Z}$$
$$\frac{\partial^2 \psi}{\partial R^2} = 2B + 4R\frac{\partial B}{\partial R} + R^2\frac{\partial^2 B}{\partial R^2}$$
$$\frac{\partial^2 \psi}{\partial Z^2} = R^2\frac{\partial^2 B}{\partial Z^2}$$
$$\frac{\partial^2 \psi}{\partial R \partial Z} = 2R\frac{\partial B}{\partial Z} + R^2\frac{\partial^2 B}{\partial R \partial Z} \tag{18}$$

Substituting into Equation (7)

$$F = 12\left(\frac{\partial B}{\partial Z}\right)^2 + 9\left(\frac{\partial B}{\partial R}\right)^2 + 12R\frac{\partial B}{\partial Z}\frac{\partial^2 B}{\partial R \partial Z} + 6R\frac{\partial B}{\partial R}\frac{\partial^2 B}{\partial R^2} - 6R\frac{\partial B}{\partial R}\frac{\partial^2 B}{\partial Z^2} - 2R^2\frac{\partial^2 B}{\partial Z^2}\frac{\partial^2 B}{\partial R^2} + R^2\left(\frac{\partial^2 B}{\partial R^2}\right)^2 + R^2\left(\frac{\partial^2 B}{\partial Z^2}\right)^2 + 4R^2\left(\frac{\partial^2 B}{\partial R \partial Z}\right)^2 \tag{19}$$

The Variational Integral

In terms of the new variable Equation (8) may be written:

$$\frac{\partial}{\partial B} \iiint F(B)\,d(volume) = 0 \tag{20}$$

In order to solve this problem, the nodal variables must be specified on the external surfaces of the volume over which the integral is to be evaluated. For axisymmetric flows in cylindrical coordinates this equation is reduced to:

$$2\pi \frac{\partial}{\partial B} \iint F(B) R\,d(area) = 0 \tag{21}$$

and the boundaries concerned $(R, 0)$, (R, ∞) and $(1, Z)$.

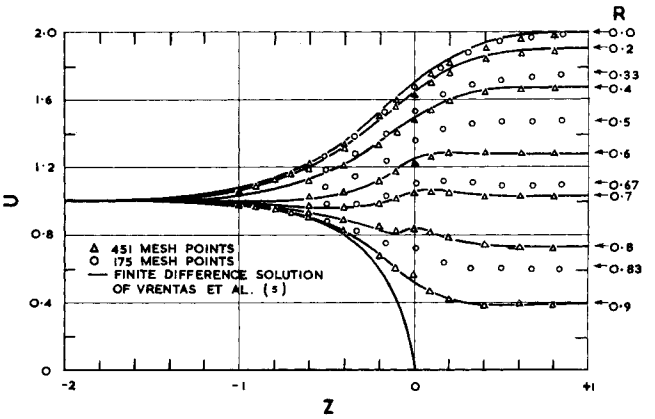

Fig. 5. Comparison between finite element and finite difference solution.

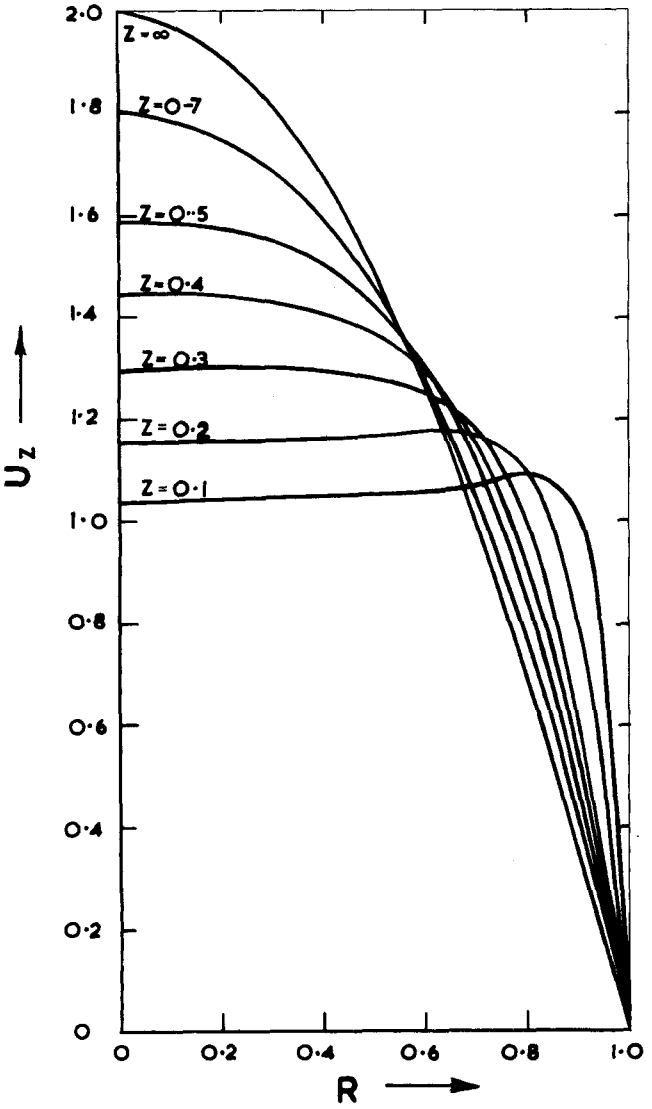

Fig. 6. Velocity profile development in a pipe for creeping flow.

Boundary Conditions

In terms of the new variable the boundary conditions given on Figure 3 become:

$Z = 0$

$$B = -\frac{1}{2}; \quad \frac{\partial B}{\partial R} = 0; \quad \frac{\partial B}{\partial Z} = 0 \qquad (22)$$

$Z = \infty$

$$B = \frac{R^2}{2} - 1; \quad \frac{\partial B}{\partial R} = R; \quad \frac{\partial B}{\partial Z} = 0 \qquad (23)$$

$R = 1$

$$B = -\frac{1}{2}; \quad \frac{\partial B}{\partial R} = 1; \quad \frac{\partial B}{\partial Z} = 0 \qquad (24)$$

NUMERICAL SOLUTIONS

The Entrance Region Problem with the Streamtube Initial Condition

Vrentas, et al. (5) have presented a creeping flow solution to the Navier-Stokes equations for the boundary conditions given on Figure 2. This solution has more recently been shown to agree with an analytical solution (17).

It is appropriate to use such a solution to confirm the applicability of the finite element method. Unfortunately this cannot be obtained for the boundary conditions given on Figure 2 as for $-\infty < Z < 0$, when R is unity, $\partial U/\partial R$ is given as zero. In terms of the stream function and the new variable B, this results in boundary conditions containing second derivatives. In order to overcome this difficulty, numerical values of $U(Z)$ were taken from the Vrentas solution as the boundary condition in this region.

The data obtained are compared with the Vrentas solution on Figure 5. The flow field used extended over Z between ± 2. Two solutions were performed using 175 and 451 mesh points respectively (138 and 390 interior points). It may be noted that even the relatively coarse mesh provides excellent agreement. The execution time required amounted to 35 and 90 min. for the two solutions using an ICT 1905 computer.

The Entrance Region Problem with the Flat Initial Condition

A solution for $U(R, Z)$ is given in Figure 6 for the boundary conditions in Equations (22), (23), and (24). The axial distance used was $0 < Z < 4$ with a total of 451 mesh points for adequate definition.

An interesting feature of the solution is the maximum in the $U(R)$ profiles similar to that produced by Wang and Longwell (4) in their parallel plate solution at a Reynolds number of 300.

EXPERIMENTAL STUDIES

The experimental study of Atkinson, et al. (9) has been extended to cover the Reynolds numbers 1.1, 3.3, 6.3, 23.2, 109, and 215, using aqueous glycerol as the experimental medium. The data are recorded on Figures 7 and 8 as a center line velocity deficiency vs. position. Superimposed on these graphs are the creeping flow solution obtained using the finite element method and the numerical data of Hornbeck (2) for the high Reynolds number asymptote. The lower limit of reasonable agreement with the boundary-layer solution can be seen to be in the region of 200, as suggested by Christiansen and Lemmon (18).

ENTRY LENGTH CORRELATION

On Figures 7 and 8 a horizontal line has been drawn corresponding to a 99% approach to fully developed flow. From this line, data corresponding to Equation (3) may

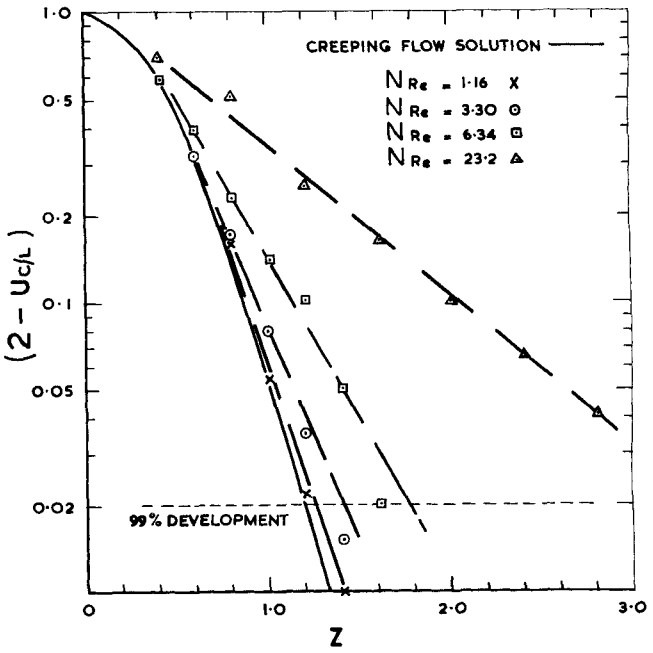

Fig. 7. Comparison of axial velocity development at finite Reynolds numbers with creeping flow solution.

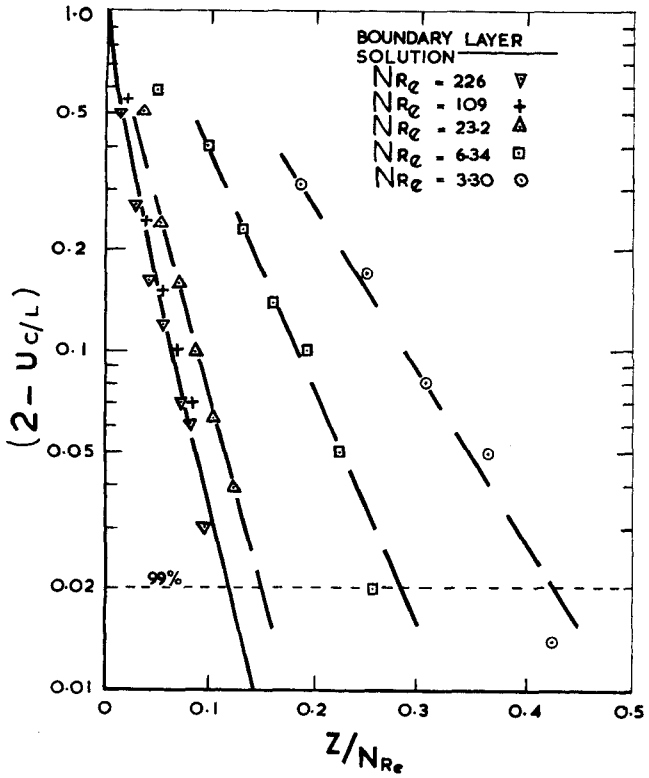

Fig. 8. Comparison of axial velocity development at low Reynolds numbers with boundary layer solution.

be obtained; these results are recorded on Figure 9. Two asymptotes are indicated as expected. Linear addition of the values of these asymptotes obtained from the numerical solutions yields:

$$Z_e = 1.18 + 0.112\,N_{Re} \tag{25}$$

This equation has been superimposed on Figure 9. It provides a satisfactory curve fit for experimental results. The small deviation may undoubtedly be explained by the fact that the profile leaving the distributor was partially developed.

For convenience of comparison, the numerical data of Vrentas when using the stream-tube initial condition have also been included.

APPLICATION TO PARALLEL PLATES

In view of the success of Equation (25) it is appropriate to provide the equivalent equation for the parallel plate situation. The high Reynolds number asymptote has been provided by Bodoia and Osterle (*1*) and the creeping flow solution obtained by the finite element method.

For axisymmetric, incompressible creeping flow in rectangular coordinates, the function F of Equation (7) becomes:

$$F = 4\left(\frac{\partial^2\psi}{\partial X\partial Y}\right)^2 + \left(\frac{\partial^2\psi}{\partial Y^2}\right)^2 + \left(\frac{\partial^2\psi}{\partial X^2}\right)^2 - 2\frac{\partial^2\psi}{\partial X^2}\frac{\partial^2\psi}{\partial Y^2} \tag{26}$$

where

$$U = -\frac{\partial\psi}{\partial Y}; \quad V = \frac{\partial\psi}{\partial X}$$

Introducing a new variable as before, this time to reduce the field from cubic to quadratic;

$$B = \frac{\psi}{Y} \tag{27}$$

Equation (26) becomes:

$$F = 4\left\{\left(\frac{\partial B}{\partial X}\right)^2 + Y^2\left(\frac{\partial^2 B}{\partial X\partial Y}\right)^2 + 2Y\frac{\partial B}{\partial X}\frac{\partial^2 B}{\partial X\partial Y}\right\} + 4\left(\frac{\partial B}{\partial Y}\right)^2 + Y^2\left(\frac{\partial^2 B}{\partial Y^2}\right)^2 + 4Y\frac{\partial B}{\partial Y}\frac{\partial^2 B}{\partial Y^2} + Y^2\left(\frac{\partial^2 B}{\partial X^2}\right)^2 - 2\left\{2Y\frac{\partial^2 B}{\partial X^2}\frac{\partial B}{\partial Y} + Y^2\frac{\partial^2 B}{\partial Y^2}\frac{\partial^2 B}{\partial X^2}\right\} \tag{28}$$

Application of Equation (20) to rectangular cartesian coordinates with a two dimensionless flow field yields:

$$\frac{\partial}{\partial B}\iint F(B)\,d(area) = 0 \tag{29}$$

In this case the nodal variables have to be specified on the four external boundaries. However, a further advantage of the transformation [Equation (27)] is that in terms of the new variable B the field is symmetrical about $Y = 0$ and consequently it is only necessary to solve for one half with restrictions specified at $(Y, 0)$, (Y, ∞), and $(1, X)$. The boundary conditions are then:

$X = 0$

$$B = -1; \quad \frac{\partial B}{\partial X} = 0; \quad \frac{\partial B}{\partial Y} = 0 \tag{30}$$

$X = \infty$

$$B = -\frac{3}{2}\left(1 - \frac{Y^2}{3}\right); \quad \frac{\partial B}{\partial Y} = Y; \quad \frac{\partial B}{\partial X} = 0 \tag{31}$$

$Y = 1$

$$B = -1; \quad \frac{\partial B}{\partial Y} = 1; \quad \frac{\partial B}{\partial X} = 0 \tag{32}$$

The solution in terms of $U(X, Y)$ is given on Figure 10 and the axial velocity deficiency curve on Figure 11. Once again the local maxima are a feature of the velocity profiles.

From Figure 11 the entrance length is obtained as 1.25 and Equation (33) provides the required relationship between entrance length and Reynolds number.

$$X_e = 1.25 + 0.088\,(N_{Re})_p \tag{33}$$

As in the previous case, this equation is the sum of the creeping flow and boundary layer solutions.

CONCLUSIONS

1. A linear combination of asymptotic solutions adequately describes the entrance region for all Reynolds

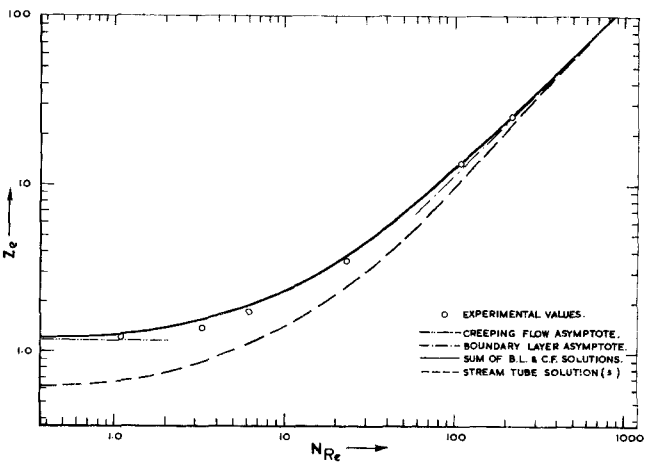

Fig. 9. 99% development entry length from flat profile as a function of Reynolds number.

numbers. This predicts a finite entry length under creeping flow conditions, a feature that is supported by experiment.

2. Maxima occur in developing velocity profiles with flat initial conditions, although in practice it is probable that these cannot be generated with sufficient accuracy for the phenomena to be detected.

NOTATION

A = area of an element
a = pipe radius
b = half width between parallel plates
B = dependent variable
P = dependent variable
r, z = cylindrical coordinates
R, Z = cylindrical coordinates ($= r/a, z/a$)
N_{Re} = Reynolds number in pipes based on diameter
$(N_{Re})_p$ = Reynolds number between parallel plates based on width
$\bar{u}$ = average velocity
U = axial velocity component ($= u/\bar{u}$)
$U_{C/L}$ = center line velocity (dimensionless)
v = transverse velocity component
V = transverse velocity component ($= v/\bar{u}$)
x, y = rectangular coodinates
X, Y = rectangular coordinates ($= x/b, y/b$)
Z_e = entrance length (dimensionless)
μ = viscosity
ρ = density
ψ = dimensionless stream function [defined in Equation (5)]

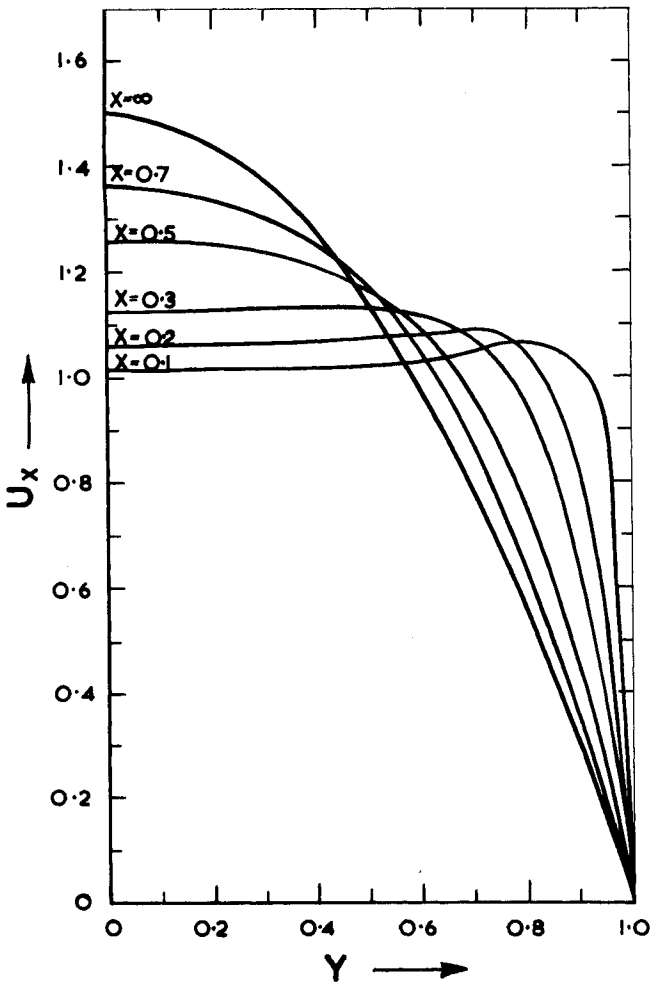

Fig. 10. Velocity profile development between parallel plates for creeping flow.

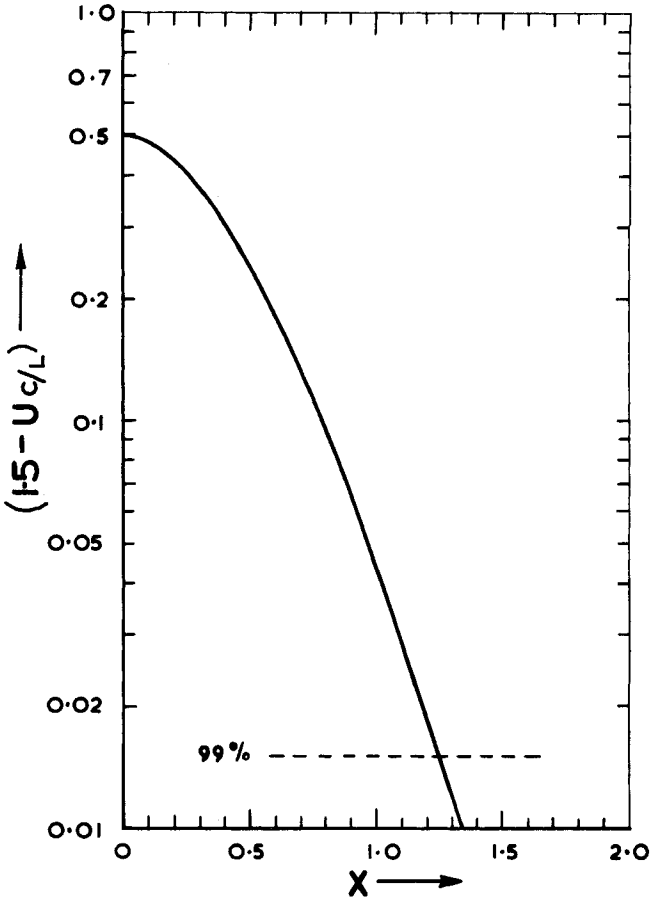

Fig. 11. Creeping flow solution for axial velocity development between parallel plates.

LITERATURE CITED

1. Bodoia, J. R., and J. F. Osterle, *Appl. Sci. Res.* **A10**, 265 (1961).
2. Hornbeck, R. W., *ibid.*, **A13**, 224 (1964).
3. Atkinson, B., and C. C. H. Card, *Inst. Chem. Eng. Symposium Ser. No. 23*, 146 (1967).
4. Wang, Y. L., and P. A. Longwell, *AIChE J.*, **10**, 323 (1964).
5. Vrentas, J. S., J. L. Duda, and K. G. Bargeron, *ibid.*, **12**, 837 (1966).
6. Prandtl, L., and O. G. Tietjens, "Applied Hydro- and Aero-mechanics," p. 25, Dover, New York (1957).
7. Reshotko, E., *Progr. Rept. No. 20-364*, Jet Propulsion Lab., California Inst. Tech., (Oct. 24, 1958).
8. Pfenniger, W., "Boundary Layer Flow and Control," G. V. Lachmann, ed., Vol. 2, p. 970, Pergamon Press, New York (1961).
9. Atkinson, B., Z. Kemblowski, and J. M. Smith, *AIChE J.*, **13**, 17 (1967).
10. Korteweg, D. J., *Phil. Mag.*, **16**, 112, (1883).
11. Lord Rayleigh, *ibid.*, **26**, 776 (1913).
12. Lamb, H., "Hydro-dynamics," 6th Ed., p. 617, Cambridge Univ. Press (1963).
13. Bird, R. B., W. E. Stewart, and E. N. Lightfoot, "Transport Phenomena," p. 91, John Wiley, New York (1960).
14. Turner, M. J., R. W. Clough, H. C. Martin, and L. J. Topp, *J. Aero. Sci.*, **23**, 805 (1956).
15. Zienkiewicz, O. C., "The Finite Element Method in Structural and Continuum Mechanics," McGraw-Hill, London (1967).
16. Card, C. C. H., Ph.D. thesis, Univ. Wales, Swansea (1968).
17. Vrentas, J. S., and J. L. Duda, *AIChE J.*, **13**, 97 (1967).
18. Christiansen, E. B., and H. E. Lemmon, *ibid.*, **11**, 995 (1965).

Manuscript received October 19, 1967; revision received April 22, 1968; paper accepted April 24, 1968.